Supplementary Information for

A Covalency-Electrostatics Crossover Sets the Eleven-Water Threshold for HF Dissociation

Enze Gao[1], Zhangzhe Hu[1], Xinyue Pan[1], Liwei Shi[1], Yixin Li[2], Chuanfu Huang[1,*]

1. School of Materials Science and Physics, China University of Mining and Technology, Xuzhou, Jiangsu 221116, China

2. Key Laboratory of Advanced Energy Materials Chemistry (Ministry of Education), Nankai University, Tianjin 300071, China

[*]Email: chuanfuh@cumt.edu.cn

Part I. Structural evolution and energetic competition in $HF(H_2O)_n$ (n = 1–10) clusters

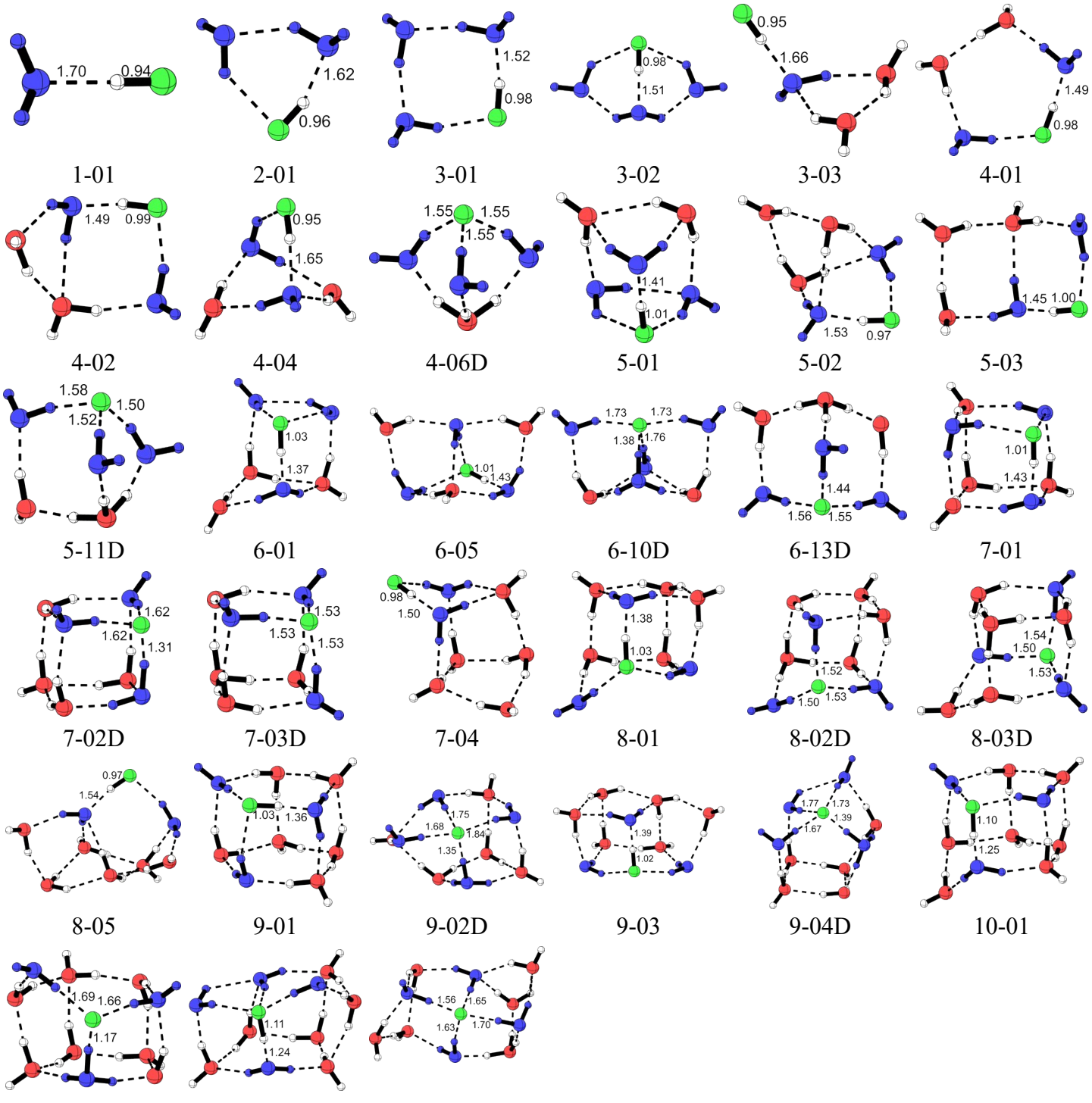

10-02D 10-03 10-05D

Fig. S1 | Selected stable structures of $HF(H_2O)_n$ (n = 1–10) optimized at the B3LYP-D3(BJ)/6-311+G(d,p) level. For each cluster size (n), up to four representative structures are shown, with an approximately balanced number of molecular and ionic motifs. Color code: H, white; F, green. For O atoms, blue denotes first-shell water molecules directly interacting with HF or F^- (including H_3O^+), whereas red denotes outer-shell water molecules. Bond lengths are given in Å.

Table S1 | Relative energies (kcal·mol^{-1}), water coordination numbers (WCN), and ion-pair types of $HF(H_2O)_n$ (n = 1–5) at the M06-2X-D3(0)/def2-TZVPD level.

Structure	ΔE_{rel}	WCN	Type	Structure	ΔE_{rel}	WCN	Type
1-01	0.00	1	–	5-01	0.00	3	–
2-01	0.00	2	–	5-02	1.60	2	–
3-01	0.00	2	–	5-03	2.02	2	–
3-02	4.42	3	–	5-04	2.58	3	–
3-03	5.44	1	–	5-05	2.65	2	–
4-01	0.00	2	–	5-06	2.84	3	–
4-02	0.13	2	–	5-07	5.12	2	–
4-03	0.70	2	–	5-08	5.67	2	–
4-04	1.56	2	–	5-09	6.11	2	–
4-05	4.39	2	–	5-10	6.60	2	–
4-06D	7.40	3	SIP	5-11D	8.11	3	SIP

As summarized in Table S1, only a limited number of isomers are found for n = 1–3, which can be attributed to the relatively simple potential-energy surfaces at these sizes, featuring fewer accessible local minima (stable conformers). A particularly notable case is the bicyclic structure 3-02, in which HF interacts with three water molecules yet remains in the molecular (undissociated) form. By contrast, for $HCl(H_2O)_3$ and $HBr(H_2O)_3$ clusters (Fig. S2), the same structural motif appears as a fully dissociated CIP, and the latter is even the GM for the HBr system.[1–3] This comparison indicates that the F atom binds the proton much more strongly than its congeners Cl and Br, consistent with fluorine being the most electronegative element.

Briefly, these comparisons indicate that HF is more prone to remain molecular in small water clusters because the H-F bond is more strongly covalent and significantly stronger, making proton transfer from F intrinsically less favorable. In contrast, the weaker H-X bonds in HCl/HBr and the higher polarizability of Cl^-/Br^- facilitate the formation and stabilization of CIPs within the same hydration framework. Consequently, HF requires a higher degree of solvation/coordination saturation to achieve thermodynamically stable dissociation, consistent with its stronger proton-binding capability (also in line with fluorine's high electronegativity).

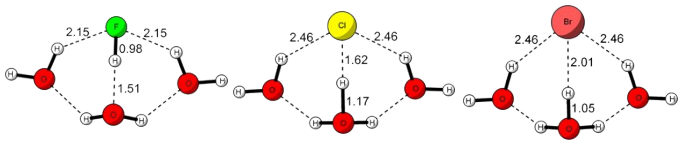

$HF(H_2O)_3$ $HCl(H_2O)_3$ $HBr(H_2O)_3$

Fig. S2 | Bicyclic structures of $HX(H_2O)_3$ (X = F, Cl, Br) optimized at the B3LYP-D3(BJ)/6-311+G(d,p) level.

At n = 4, the smallest dissociated $HF(H_2O)_n$ structure currently identified, 4-06D, emerges. This

motif corresponds to a SIP and lies as high as 7.40 kcal·mol^{-1} in relative energy, making it the least stable isomer of $HF(H_2O)_4$. A similar trend is found at n = 5: the dissociated structure 5-11D is also a SIP and sits at the top of the energy ladder for this size with a relative energy of 8.11 kcal·mol^{-1}. These results indicate that, in very small water clusters, HF dissociation preferentially yields SIPs, whereas CIPs are not observed.

Table S2 | Relative energies (kcal·mol^{-1}), WCN, and ion-pair types of $HF(H_2O)_n$ (n = 6,7) at the M06-2X-D3(0)/def2-TZVPD level.

Structure	ΔE_{rel}	WCN	Type	Structure	ΔE_{rel}	WCN	Type
6-01	0.00	3	–	7-01	0.00	3	–
6-02	0.31	3	–	7-02D	1.98	3	CIP
6-03	0.36	3	–	7-03D	4.08	3	SIP
6-04	1.05	3	–	7-04	5.05	2	–
6-05	1.38	3	–	7-05	5.80	3	–
6-06	1.67	3	–	7-06	7.28	2	–
6-07	2.52	3	–	7-07	7.67	2	–
6-08	2.95	3	–	7-08	8.06	2	–
6-09	3.07	2	–	7-09	8.42	2	–
6-10D	3.46	4	CIP	7-10	8.53	3	–
6-11	3.95	3	–	7-11	8.70	4	–
6-12D	7.21	3	SIP	7-12	9.25	2	–
6-13D	8.60	3	SIP	7-13D	14.55	3	SIP

As shown in Table S2, more dissociated motifs emerge at n = 6 and 7, including the first appearance of CIPs. Nevertheless, the molecular clusters remain thermodynamically more stable overall. For instance, 6-05 (molecular) and 6-10D (CIP) in Fig. S1 share a similar structural framework, yet the molecular isomer 6-05 is still more stable by 2.08 kcal·mol^{-1}. The same trend persists at n = 7: although the canonical cubic framework is intrinsically stable, the molecular cube 7-01 lies markedly lower in energy than its dissociated cubic variants, namely the CIP (7-02D) and SIP (7-03D) isomers. Collectively, these results indicate that under the present hydration conditions, HF preferentially remains stable in its molecular form.

Table S3 | Relative energies (kcal·mol^{-1}), WCN, and ion-pair types of $HF(H_2O)_n$ (n = 8–10) at the M06-2X-D3(0)/def2-TZVPD level.

Structure	ΔE_{rel}	WCN	Type	Structure	ΔE_{rel}	WCN	Type
8-01	0.00	3	–	9-01	0.00	3	–
8-02D	2.45	3	SIP	9-02D	2.97	4	CIP
8-03D	3.25	3	SIP	9-03	3.32	3	–
8-04D	4.72	3	CIP	9-04D	4.03	4	CIP
8-05	5.02	2	–	9-05	4.70	2	–
8-06	5.22	3	–	9-06	4.89	3	–
8-07D	5.41	3	SIP	9-07	5.24	3	–
8-08	5.67	3	–	9-08	5.26	4	–
8-09	5.69	2	–	9-09	5.29	3	–
8-10	5.76	3	–	9-10	5.57	3	–

8-11	5.91	3	–	9-11D	6.28	3	CIP
8-12	5.93	2	–	9-12D	6.60	4	CIP
8-13	6.62	2	–	9-13D	7.84	3	CIP
10-01	0.00	3	–	10-08D	5.05	4	SIP
10-02D	0.29	3	CIP	10-09D	5.16	4	SIP
10-03	1.82	4	–	10-10D	5.19	3	–
10-04	3.37	3	–	10-11	5.91	3	–
10-05D	4.57	4	SIP	10-12D	6.03	5	SIP
10-06D	4.67	3	CIP	10-13	6.20	3	–
10-07	4.83	3	–	10-14	6.21	3	–

From Table S3, increasing the number of water molecules to n = 8–10 leads to a concomitant rise in the number of dissociated motifs. Nevertheless, molecular clusters remain thermodynamically more stable at all sizes. For example, the pairs (8-01/8-02D) and (10-01/10-02D) share similar geometric frameworks, yet the molecular counterparts consistently lie lower in energy. Notably, at n = 10 the energy gap between the dissociated isomer 10-02D and the most stable molecular structure 10-01 is only 0.29 kcal·mol^{-1}. This value is much smaller than the corresponding gap at n = 7 (1.98 kcal·mol^{-1}) and is significantly smaller than any gap observed for $n \leqslant 9$. These results suggest that at n = 10 the system approaches the critical size at which HF can undergo thermodynamically stable dissociation.

Part II. Representative IR spectra of paired molecular and ionic isomers at n = 11 and 12

To provide a direct comparison between molecular and ionic isomers at the critical sizes, we further simulated the IR spectra of two representative structural pairs, namely 11-01D/11-04 and 12-01D/12-13 (Fig. S3). These pairs have closely related hydrogen-bond backbones but different proton-transfer states, making them suitable for identifying the spectral changes induced by HF dissociation. In this comparison, the red and green peaks are used to track the molecular HF-related vibrational features, whereas the blue peaks are used to identify proton-involving vibrational features associated with the ionically dissociated structures.

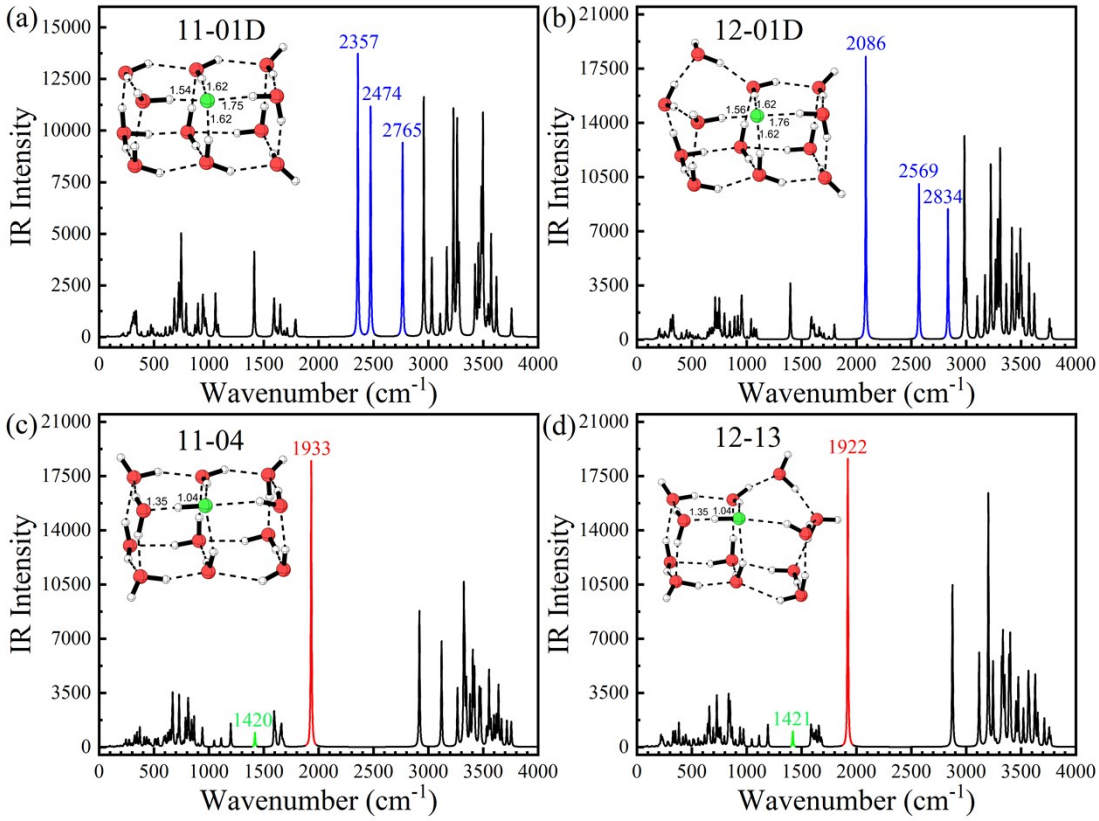

Fig. S3 | Simulated IR spectra of paired ionic and molecular $HF(H_2O)_n$ isomers at n = 11 and 12. The spectra were simulated at the B3LYP-D3(BJ)/6-311+G(d,p) level, using a scaling factor of 0.9688 for the harmonic frequencies. Panels (a,c) compare 11-01D and 11-04, whereas panels (b,d) compare 12-01D and 12-13. Insets show the optimized geometries, with selected F⁻···H distances labelled for the ionic structures and F-H/H···O distances labelled for the molecular structures. Red, green and blue peaks denote the H-F stretching vibration, the in-plane wagging motion of the H atom within the F-H···O hydrogen bond, and H_3O^+-related proton-involving vibrational features, respectively.

For the n = 11 pair, the molecular structure 11-04 retains a short F-H distance of 1.04 Å and an H···O distance of 1.35 Å, indicating that HF remains in a strongly hydrogen-bonded but undissociated form. Consistent with this structural feature, its IR spectrum shows a red-labelled band at 1933 cm^{-1} and a green-labelled band at 1420 cm^{-1}. The former corresponds to the strongly red-shifted H-F stretching vibration, whereas the latter corresponds to the in-plane wagging motion of the H atom of HF relative to the neighbouring H_2O molecule within the F-H···O hydrogen bond. In contrast, in the ionic structure 11-01D, these molecular HF-related red and green bands are no longer present. Instead, three new features highlighted in blue emerge at 2357, 2474 and 2765 cm^{-1}. From low to high frequency, these bands can be assigned to the back-and-forth shuttling motion of the proton between two out-of-plane wagging H_2O molecules, the antisymmetric stretching of the three O-H bonds in the hydronium ion H_3O^+, and its symmetric O-H stretching mode, respectively. This paired comparison

shows that the proton transfer from HF to the water network leads to the disappearance of the original molecular HF features and the emergence of H_3O^+-related vibrational signatures.

A similar spectral contrast is observed for the n = 12 pair. The molecular structure 12-13 also remains in an undissociated F-H···O motif, with an F-H distance of 1.04 Å and an H···O distance of 1.35 Å. Accordingly, its spectrum retains a red-labelled H-F stretching band at 1922 cm^{-1} and a green-labelled in-plane wagging band at 1421 cm^{-1}, closely resembling the molecular features observed for 11-04. By contrast, in the ionic structure 12-01D, the red and green bands associated with molecular HF disappear completely. Meanwhile, three blue features appear at 2086, 2569 and 2834 cm^{-1}, corresponding to proton-dominated vibrational motions in the H_3O^+-containing ion-pair structure. The close analogy between the 11-01D/11-04 and 12-01D/12-13 comparisons indicates that molecular and ionic isomers exhibit a qualitative difference in their IR spectral features in the n = 11–12 size range.

Overall, these paired spectra show that HF dissociation is accompanied by an on/off-type change in the characteristic IR features. Molecular isomers retain the strongly red-shifted H-F stretching band and the F-H···O in-plane wagging band, whereas ionic isomers lose these molecular HF-related red/green bands and instead exhibit three proton-involving blue features in the 2000–3000 cm^{-1} region. This result further supports the spectral assignments made in the main text and confirms that the disappearance of the red/green bands together with the emergence of H_3O^+-related blue features is a reliable spectroscopic indicator of HF auto-dissociation into an F^-/H_3O^+ ion pair.

Part III. Energy decomposition analysis (EDA) of the interfragment interaction energy (ΔE_{int})

To further resolve the microscopic origin of the bimodal ΔE_{int} distribution and the abrupt upward jump of the global-minimum (GM) trajectory at n = 11 shown in Fig. 5 of the main text, we applied the sobEDAw scheme to decompose the interfragment interaction energy into four components, including electrostatics, exchange (Pauli repulsion), orbital interaction, and dispersion (Fig. S4).[4,5]

$$\Delta E_{int} = E_{els} + E_{exp} + E_{orb} + E_{disp}$$

First, the orbital interaction energy (E_{orb}) is identified as the decisive factor responsible for the energetic stratification. As shown in Fig. S4c, the undissociated molecular motifs (green) exhibit exceptionally strong orbital stabilization (-100 ~ -170 kcal·mol^{-1}), which directly originates from the intact covalent H-F bond. In contrast, for dissociated ionic motifs (blue), the E_{orb} contribution drops sharply upon covalent bond cleavage to the -60 ~ -100 kcal·mol^{-1} range, with most points clustered near -60 kcal·mol^{-1}. This pronounced bimodal distribution mirrors the overall ΔE_{int} stratification shown in Fig. 5 of the main text, demonstrating that E_{orb} governs the energy layering among isomers. Moreover, the red arrows in Fig. S4c trace the evolution of the GMs: an abrupt "upward jump" also occurs at n = 11, visually highlighting the covalent price that must be paid to achieve thermodynamically stable dissociation (a substantial loss of orbital stabilization, ≈ 100 kcal·mol^{-1}).

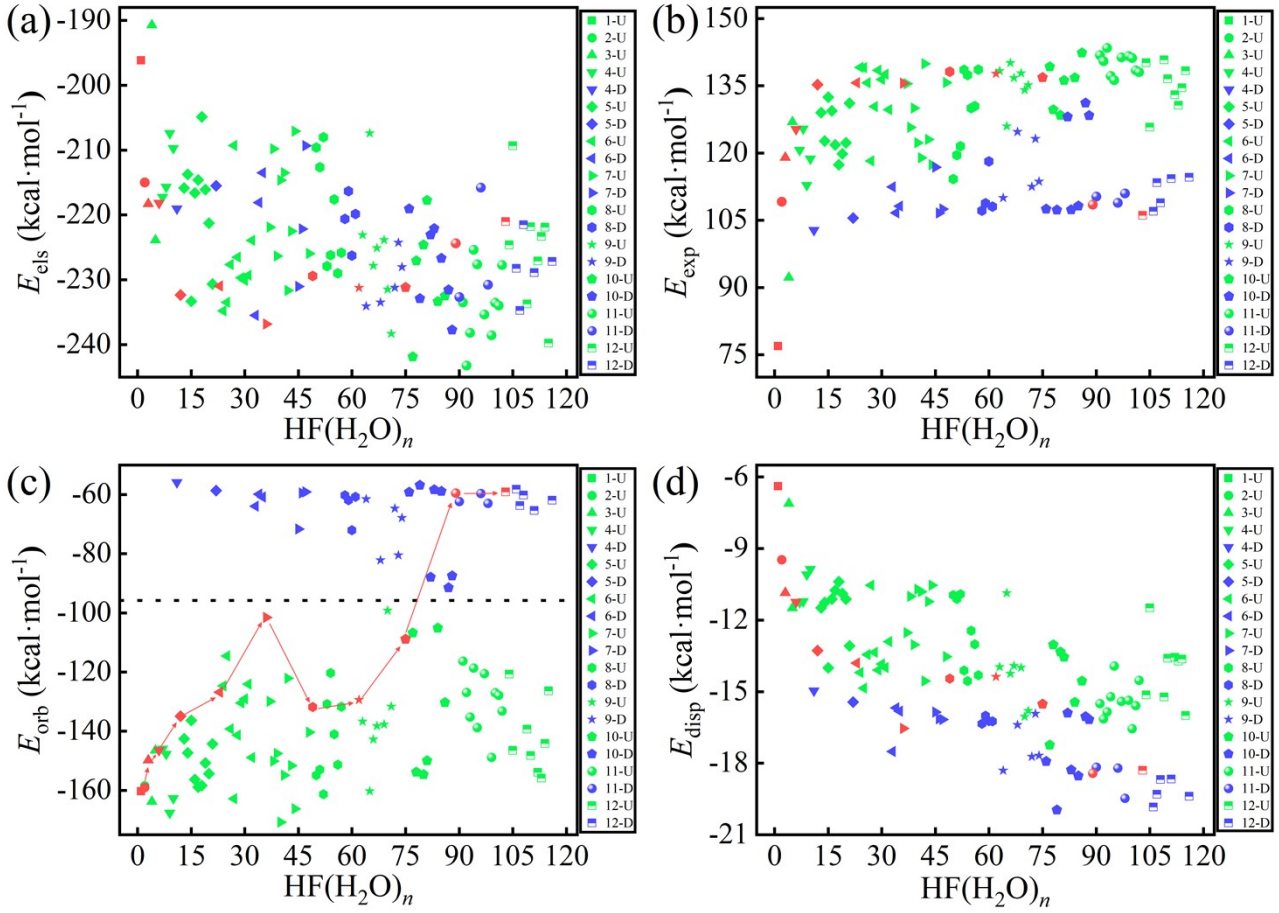

Fig. S4 | sobEDAw decomposition of the interfragment interaction energy (ΔE_{int}) between F^- and $H_3O^+(H_2O)_{n-1}$. (a) Electrostatic term (E_{els}); (b) exchange repulsion (E_{exp}, Pauli repulsion); (c) orbital interaction (E_{orb}); (d) dispersion (E_{disp}). In the legend, "n-U" denotes undissociated clusters (green) and "n-D" denotes dissociated clusters (blue). Red symbols connected by a line trace the evolution of the global-minimum structure at each cluster size. The horizontal black dashed line in panel (c) highlights the pronounced stratification in E_{orb} between the two motifs.

A natural question then arises: why can the ionic motif become the GM despite paying such a large price in orbital stabilization? The exchange repulsion term (E_{exp}) in Fig. S4b provides a key explanation. At the same cluster size n, the shorter H-F bond in the molecular motif indeed yields strong orbital attraction, but it inevitably incurs substantial Pauli repulsion (green points populate the high-energy region). In contrast, upon dissociation the H···F separation increases markedly, which releases a significant fraction of this repulsion (blue points shift to the low-energy region). This reduction in E_{exp} therefore compensates, to a large extent, for the loss in E_{orb}.

In addition, Fig. S4a shows that the electrostatic term (E_{els}) is the dominant attractive contribution for both motifs (-200 ~ -240 kcal·mol^{-1}), indicating that electrostatic attraction remains the primary driving force stabilizing the clusters in both the molecular and ionic forms. By contrast, the dispersion contribution (E_{disp}) increases approximately linearly with cluster size (Fig. S4d) and is comparatively small in magnitude, providing only a minor discriminatory contribution to the structural motif.

In summary, the component-resolved EDA results show that the emergence of the ionic GM for $n \geqslant 11$ is enabled by a cooperative compensation mechanism. Although dissociation incurs a substantial loss of orbital stabilization, this penalty is offset to a large extent by the release of Pauli repulsion, while the saturated coordination environment (WCN = 4) further stabilizes the ionic motif. Together, these effects provide the microscopic physical basis for the thermodynamically stable dissociation of HF in larger water clusters.

(1) Wang, J.; Zhuang, L.; Gao, E.; Zhang, H.; Wan, J.; Huang, C. Dissociation of HBr in Water Clusters Based on a Hybrid Density Functional Approach. *J. Phys. Chem. A* **2024**, *128* (35), 7364–7374. https://doi.org/10.1021/acs.jpca.4c02966.

(2) Odde, S.; Mhin, B. J.; Lee, S.; Lee, H. M.; Kim, K. S. Dissociation Chemistry of Hydrogen Halides in Water. *J. Chem. Phys.* **2004**, *120* (20), 9524–9535. https://doi.org/10.1063/1.1711596.

(3) Tachikawa, M. Isotope Effect and Cluster Size Dependence for Water and Hydrated Hydrogen Halide Clusters: Multi-Component Molecular Orbital Approach. *Mol. Phys.* **2002**, *100* (6), 881–901. https://doi.org/10.1080/00268970110099602.

(4) Lu, T.; Chen, Q. Simple, Efficient, and Universal Energy Decomposition Analysis Method Based on Dispersion-Corrected Density Functional Theory. *J. Phys. Chem. A* **2023**, *127* (33), 7023–7035. https://doi.org/10.1021/acs.jpca.3c04374.

(5) Su, P.; Li, H. Energy Decomposition Analysis of Covalent Bonds and Intermolecular Interactions. *J. Chem. Phys.* **2009**, *131* (1), 14102. https://doi.org/10.1063/1.3159673.